



EFFECT OF PRESSURE AND VOLTAGE ON SPHERICAL PLASMA FOCUS DYNAMICS

Yasar AY^{1,*}

¹ Department of Electrical and Electronics Engineering, Faculty of Engineering, Dicle University, Diyarbakir, Turkey

ABSTRACT

A spherical plasma focus device with two concentric electrodes is simulated using deuterium and tritium mixture (50:50) as a working gas. The developed model is used to study the effect of gas pressure and charging voltage on dynamics of current sheath in spherical plasma focus. While charging voltage is varied from 15 kV to 30 kV to see the effect of voltage, gas pressure is increased from 1 Torr to 20 Torr for gas pressure study. In this work, it is found that there is a strong correlation between current sheath dynamics and investigated parameters which are gas pressure and charging voltage.

Keywords: Current sheath, Charging voltage, Discharge current, Gas pressure, Plasma focus

1. INTRODUCTION

Plasma focus (PF) devices can generate hot and dense plasma by gas discharge, followed by the axially symmetric current sheath (CS) formation. Lorentz Force then accelerates CS until it reaches axis of PF. PF devices can be used for x-ray production [1, 2], neutron production [1, 3, 4], and nuclear fusion reactions [5, 6].

Gas pressure and charging voltage have considerable effects on the CS dynamics, x-ray emission, and neutron production in PF devices. Singh et al. investigated the effect of the gas pressure in a cylindrical PF on CS dynamics and neutron yield from PF [7]. It is found that increasing gas pressure decreases plasma speed and maximum pinch temperature but an increase in gas pressure results in increasing neutron production until some gas pressure value. Beyond this value, neutron yield starts to decrease in PF.

Etaati et al. studied the effect of gas pressure on soft and hard x-ray production from PF devices [8]. This study shows that x-ray emission increases with pressure until the optimum gas pressure value because of the increase in the density of the pinch plasma. But beyond this optimum pressure, x-ray emission decreases. At the beginning with enough current flowing in plasma, increasing gas pressure results in increasing plasma density that gives rise to higher x-ray production until optimum gas pressure. After this optimum pressure, increasing pressure gives rise to a decrease for quality of focus action of plasma focus device which results in a decrease in the electron beam energy.

Three pressure regimes were also found in terms of x-ray production in a 3 kJ, 15 kV PF device with copper anode [9]. In the first pressure regime (below 0.6 mbar), there are weak plasma x-rays and weak line radiation from copper anode. In the second pressure regime (0.6-1.5 mbar), there is intense x-ray emission with significant line radiation contribution from copper anode. In the third pressure regime (1.5-3.0 mbar), while plasma x-rays are intense, x-rays from copper anode are weak.

Roomi et al. investigated effect of the voltage and operating pressure on the soft and hard x-ray production using nitrogen as a working gas [10]. It is found that soft x-ray and hard x-ray emissions

from the plasma focus device have different optimum conditions. The plasma focus device can be optimized either for a soft x-ray or hard x-ray emission even though the intensity of both soft x-rays and hard x-rays increases with increasing voltage. It is also found that x-ray emission from the PF device has a strong correlation with charging voltage and gas pressure.

An MHD model for SPF has been developed and validated [11, 12]. Then this model is used for neutron optimization study [13, 14] and cathode radius study [15]. The main goal here is to study the effect of pressure and charging voltage on spherical plasma focus (SPF) dynamics. In this study, discharge current, discharge voltage, plasma velocity, shock velocity, plasma resistance, and magnetic field are investigated with respect to gas pressure and charging voltage variations. While the investigated range in this study for gas pressure is 1-20 Torr with 1 Torr increment, it is 15-30 kV with 1 kV increment for charging voltage study.

2. SPHERICAL PLASMA FOCUS MODEL

The developed MHD model has 4 phases: rundown phase I, rundown phase II, reflected shock phase and radiative phase. In the model, snowplow model and shock wave equations are used, and they are coupled with circuit equations to describe SPF. Figure 1 shows SPF configuration and equivalent circuit model.

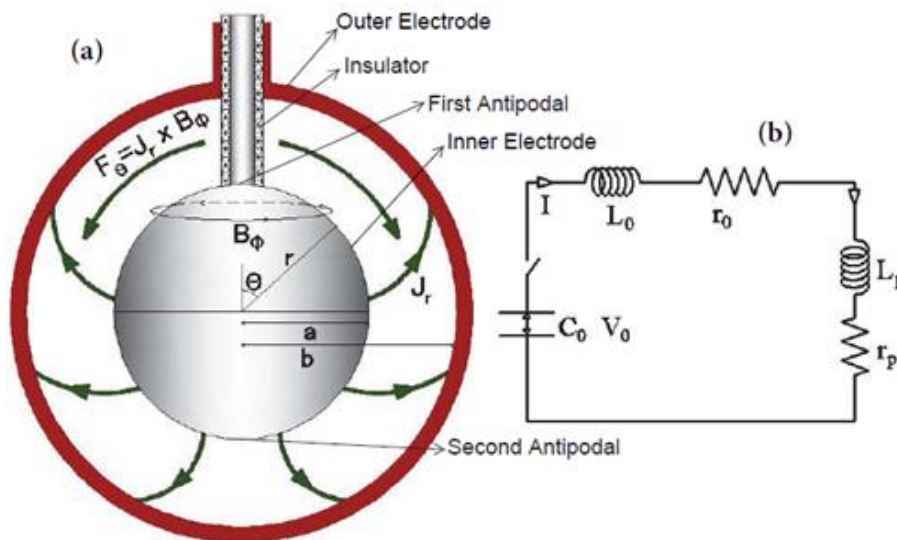


Figure 1. (a) SPF configuration, (b) equivalent circuit model

Current sheath is generated by gas discharge between anode and cathode over insulator surface and the current sheath is accelerated (rundown phase I), and then it is compressed after CS passes equator point of SPF (rundown phase II). Since CS is supersonic, an ionizing shock wave (shock front that moves faster than current sheath) is formed in front of the current sheath. After shock front hits axis of SPF, it moves back to CS (reflected shock phase), to produce pinch (high density-high temperature plasma) (radiative phase). Rundown phase I begins with current sheath formation and ends when CS reaches the equator point of device. Then rundown phase II begins. This phase ends when the shock front reaches the axis that starts the reflected shock phase. The reflected shock phase ends when reflected shock front hits coming CS that starts the last phase (radiative phase), which ends with plasma disruption at maximum compression.

A detailed theory of the model with the derivation of the equations and validation of the model were explained in previous works [11, 12]. Therefore, only brief information about the model and results produced by the developed model are discussed in this paper.

The magnetic force F_2 on current sheath results in the momentum change rate F_1 on CS. Therefore, F_1 is set equal to F_2 , which is then solved for the equation of motion. F_1 and F_2 are given as follows:

$$F_1 = \frac{d(mv_\theta)}{dt}$$

$$F_2 = \int_a^b P_B dA = \int_a^b \frac{B^2}{2\mu_0} dA$$

Where v_θ is tangential velocity, m is the mass of the plasma sheath, B is the magnetic field at distance r due to current I flowing in the CS. P_B and μ_0 are the magnetic pressure and permeability of free space. $dA = 2\pi r \sin(\theta) dr$ is the small area of the sheath. After setting F_1 equal to F_2 and solving for $\ddot{\theta}$, the equation of motions ($\ddot{\theta}$) for the rundown phase I, rundown phase II, reflected shock phase, and radiative phase are calculated as follows:

Equation of motion for rundown phase I:

$$\ddot{\theta} = \frac{\alpha^2 I^2}{r \sin \theta (\cos \theta_0 - \cos \theta)} - \frac{\dot{\theta}^2 \sin \theta}{\cos \theta_0 - \cos \theta}$$

Equation of motion for rundown phase II and reflected shock phase:

$$\ddot{\theta} = \frac{\alpha^2 I^2}{r \cos(\theta - \pi/2) (\cos \theta_0 - \cos \theta)} - \frac{\dot{\theta}^2 \sin \theta}{\cos \theta_0 - \cos \theta}$$

Where α is the scaling parameter which is given by

$$\alpha^2 = \frac{3\mu_0 f_c^2 \ln(b/a)}{8\pi^2 \rho f_m (b^3 - a^3)}$$

f_c and f_m are the current fraction that accounts for the current shedding and mass fraction swept up by the sheath motion. a and b are the inner and outer electrode radii. ρ is the initial gas density. θ_0 and θ are the angles corresponding to the insulator volume and the polar angle, respectively.

Equation of the motion for radiative phase:

$$\ddot{\theta} = \frac{\alpha^2 I^2}{r \cos(\theta - \pi/2) C} - \frac{\sin \theta \dot{\theta}^2}{C} - \frac{3QA}{2\pi \rho f_m (b^3 - a^3) r C}$$

Where $C = \cos \theta_0 - \cos \theta$, Q is the total plasma energy density.

Shock velocity for rundown phase I, rundown phase II, and reflected shock phase can be written as follows:

Shock velocity for rundown phase I:

$$v_s = -\frac{I f_c}{4\pi r \sin \theta} \sqrt{\frac{\mu_0 (\gamma + 1)}{\rho f_m}}$$

Shock velocity for rundown phase II:

$$v_s = -\frac{If_c}{4\pi r \cos\left(\theta - \frac{\pi}{2}\right)} \sqrt{\frac{\mu_0(\gamma + 1)}{\rho f_m}}$$

Shock velocity for reflected shock phase:

$$v_s = 0.3 (v_s)_{on-axis}$$

Where minus signs represent the motion in the opposite direction, γ is the specific heat ratio, $(v_s)_{on-axis}$ represents the velocity of the shock front when the shock front hits the axis at the end of the rundown phase II. The plasma temperature in Kelvin can be calculated using the shock velocity for rundown phase I and II, and the reflected shock phase as follows:

$$T = \frac{2M(\gamma - 1)}{R_0(\gamma + 1)^2} \frac{v_s^2}{(1 + Z_{eff})D_N}$$

Where M is the molecular weight, R_0 is the universal gas constant, Z_{eff} is the effective charge of the plasma, D_N is dissociation number.

Plasma resistance is calculated as follows:

$$R = \frac{\rho_{res} \times L_{col}}{A_{col}}$$

Where L_{col} is the plasma column length, $A_{col} = 2\pi a^2(1 - \cos\theta)$ is the cross sectional area of the plasma column. ρ_{res} is Spitzer resistivity.

3. RESULTS AND DISCUSSIONS

Concentric SPF is used in present work. This device has 8 cm inner (anode) and 14.5 cm outer (cathode) electrode radius. The capacitor bank and the external inductance of the SPF are 432 μ F and 36 nH, respectively. The charging voltage is 25 kV, and the DT (50:50) gas mixture pressure is 14.5 Torr. In this study, the effects of gas pressure variations (from 1 Torr to 20 Torr with 1 Torr increment) and charging voltage variations (from 15 kV to 30 kV with 1 kV increment) on current sheath dynamics are investigated. Charging voltage of 25 kV is used for the investigation of the pressure variations effect on the CS dynamics while the gas pressure is kept at 14.5 Torr (1:1 DT mixture) for studying voltage variations effect on the CS dynamics.

Figure 2 and Figure 3 show discharge currents for pressure and voltage variations. While "Max I" represents maximum discharge current value, "Dip I" represents current dip of discharge current. Increasing gas pressure or charging voltage will results in increase in discharge current. While the relation between charging voltage and discharge current is more linear, discharge current is reaching some maximum value (1500 kA) for pressure increase, which is an indication of the fact that there is an optimum pressure value for discharge current increase with respect to gas pressure. While difference between "Max I" and "Dip I" increases in Figure 2, it is not changing that much for Figure 3. The difference between "Max I" and "Dip I" in Figure 2 and Figure 3 show the value of the current dip. Deeper current dip is one of the indicators for better focus in PF devices. Therefore, increasing gas pressure until some optimum value will result in better focusing action in spherical plasma focus. While discharge current reaches 1500 kA for pressure increase, it is 1600 kA for voltage increase in this study.

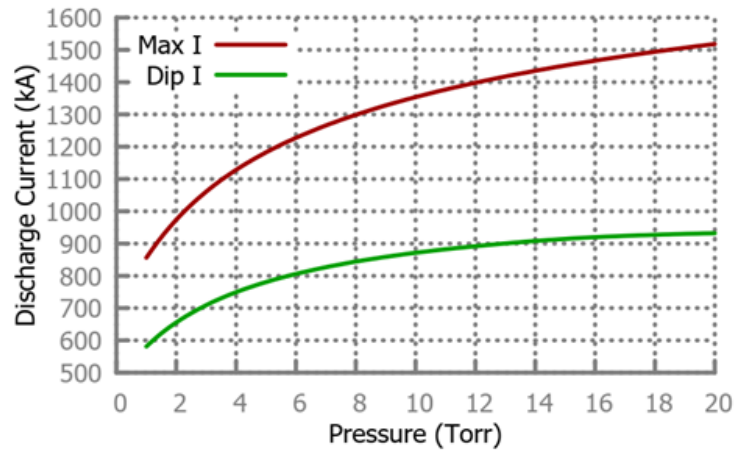


Figure 2. Discharge current for pressure variations

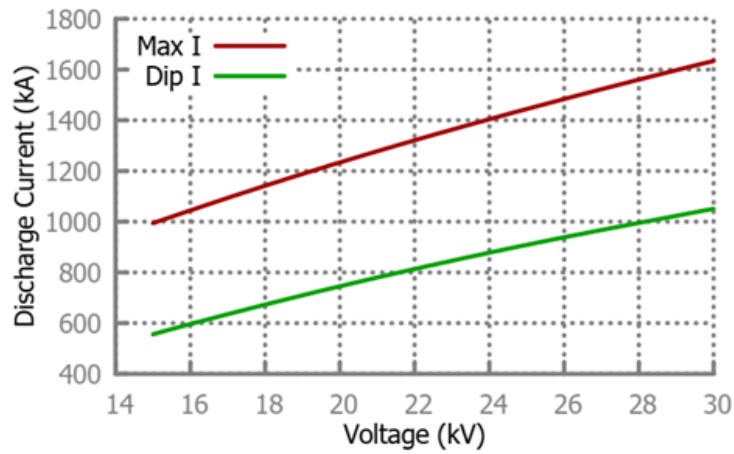


Figure 3. Discharge current for voltage variations

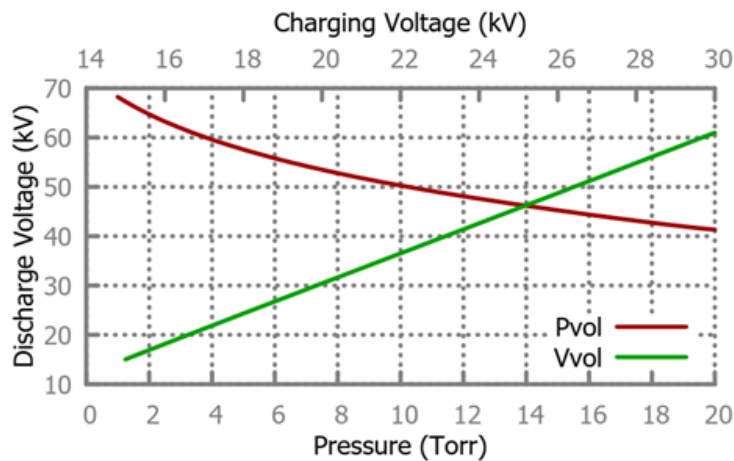


Figure 4. Discharge voltage

Discharge voltage with respect to gas pressure and charging voltage can be seen in Figure 4. In this figure, Pvol and Vvol represent discharge voltage with respect to pressure and charging voltage, respectively. Discharge voltage is increasing with charging voltage but decreasing with gas pressure.

For the charging voltage variations with 14.5 Torr gas pressure, the discharge voltage is around 15 kV with 15 kV charging voltage and it increases to 60 kV with 30 kV charging voltage. For the gas pressure variations with 25 kV charging voltage, discharge voltage is around 70 kV with 1 Torr pressure in the beginning and then decreases to 40 kV with 20 Torr gas pressure.

Figure 5 and Figure 6 show the plasma and shock velocity for pressure and voltage variations, respectively. While Pvel and Vvel represent plasma velocity with respect to pressure and voltage variations, PSvelo and VSvelo represent shock velocity with respect to pressure and voltage variations. As can be seen in this figures, pressure and voltage have similar effect on plasma and shock velocities. Both shock velocity and plasma velocity increase with increasing charging voltage but increasing gas pressure decreases plasma and shock velocities. While maximum plasma velocity is 11.3 cm/μs with 25 kV charging voltage and 1 Torr gas pressure, maximum shock velocity is 17.4 cm/μs with the same parameters.

As can be seen in Figure 5 and Figure 6, gas pressure variations has a stronger effect on plasma and shock velocity than charging voltage variations. For the plasma resistance in Figure 7, it is quite the opposite. The effect of the voltage variations on plasma resistance is stronger than the pressure variations effect. Here Pres and Vres represent plasma resistance with respect to pressure and voltage variations.

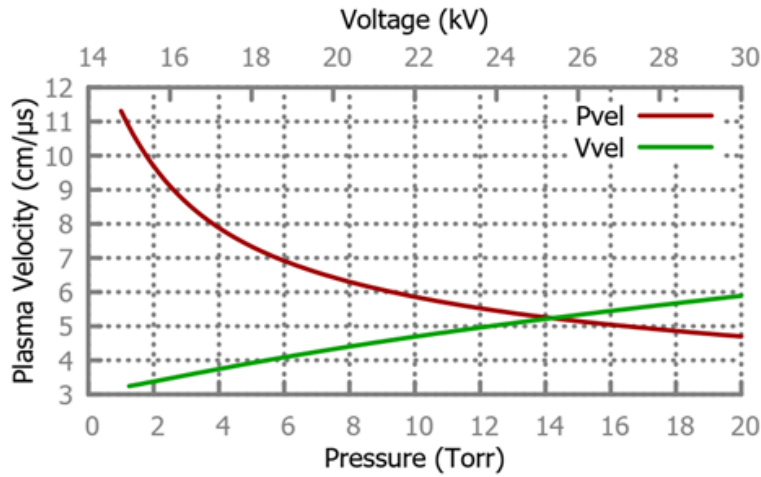


Figure 5. Plasma velocity

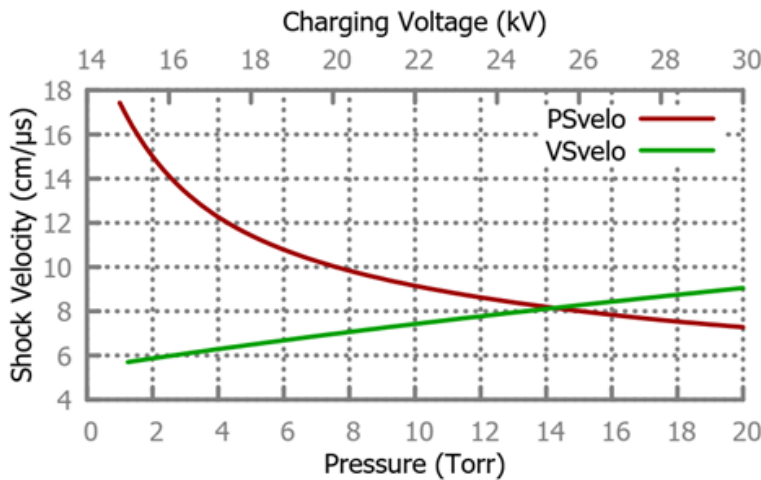


Figure 6. Shock velocity

Figure 7 shows that increasing gas pressure increases the plasma resistance while voltage increase results in decreasing plasma resistance.

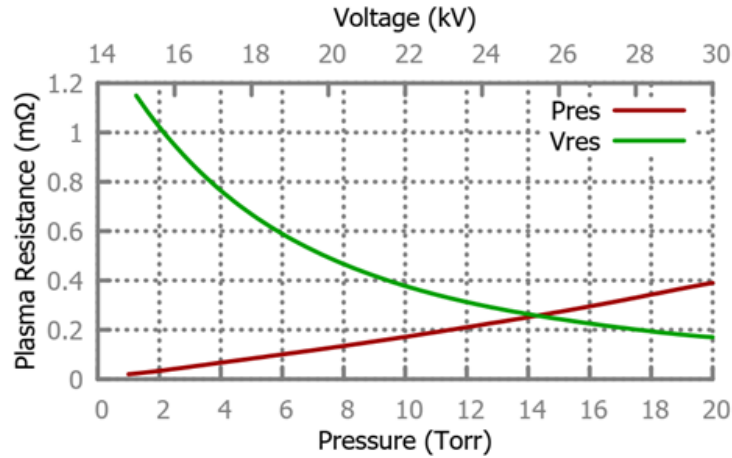


Figure 7. Plasma resistance

Figure 8 shows the magnetic field with respect to pressure and voltage. The magnetic field is increasing with both pressure and voltage increase. While increasing charging voltage increases the magnetic field almost linearly, magnetic field reaches some optimum value with pressure increase as in the pressure effect on the discharge current.

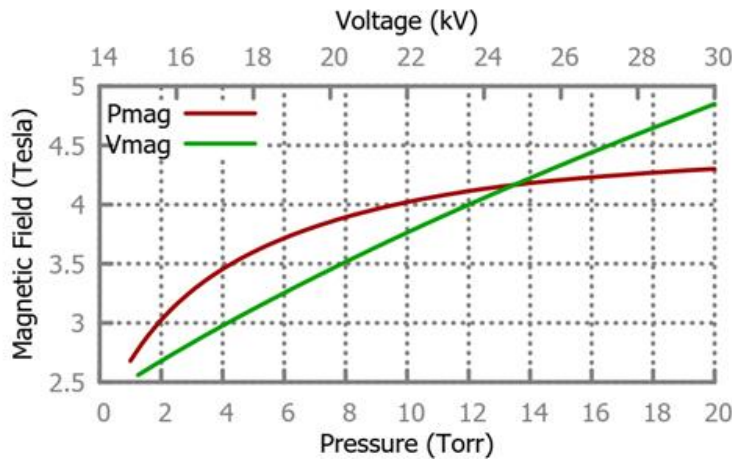


Figure 8. Magnetic field

3. CONCLUSIONS

In this work, it is found that gas pressure and charging voltage have a significant effect on CS dynamics in the SPF device in that variations of the pressure and voltage effect directly discharge current, discharge voltage and other plasma parameters. Therefore, these variations would result in various neutron yield, x-ray production and ion production in the spherical plasma focus device. Discharge current, discharge voltage, plasma and shock velocity, plasma resistance and magnetic field are investigated with respect to gas pressure and charging voltage variations in SPF.

While increasing charging voltage increases discharge current proportionally, the rate of increase in discharge current decreases with increasing gas pressure. It is also found that pressure increase results in an exponential decrease in charging voltage, plasma velocity and shock velocity, voltage increase leads to a linear increase for these parameters. For future works, effect of the pressure and voltage on

neutron yield and radiation emission in the spherical plasma focus would be beneficial in order to have more insight for these two effects on plasma focus devices. In addition, gases other than hydrogen, deuterium and tritium can be investigated in the spherical plasma focus device as the working gases.

ACKNOWLEDGMENTS

This work was supported by The Scientific and Technological Research Council of Turkey, Project No: 119F039

REFERENCES

- [1] Zakaullah M, Murtaza G, Qamar S, Ahmad I, Beg M. Neutron and x-ray emission studies in a low energy plasma focus. *Physics Scripta* 1996; 53(3): 360.
- [2] Zakaullah M, Ahmad I, Murtaza G, Beg M. Influence of magnetic probe presence on current sheath Dynamics in plasma focus operation. *Fusion Engineering and Design* 1997; 36(4): 437-446.
- [3] Lee S, Saw SH. Neutron scaling laws from numerical experiments. *Journal of Fusion Energy* 2008; 27(4): 292-295.
- [4] Serban A, Lee S. Experiments on speed-enhanced neutron yield from a small plasma focus. *Journal of Plasma Physics* 1998; 60(1): 3-15.
- [5] Pouzo J, Milanese M. Applications of the dense plasma focus to nuclear fusion and plasma astrophysics. *IEEE Transactions on Plasma Science* 2003; 31(6): 1237-1242.
- [6] Zaeem AA. Effect of the drive parameter on the differential fusion products in plasma focus devices. *IEEE Transactions on Plasma Science* 2010; 38(8): 2069-2073.
- [7] Singh A, Sing L, Saw SH. Effect of the variation of pressure on the Dynamics and neutron yield of plasma focus machines. *IEEE Transactions on Plasma Science* 2017; 45(8): 2286-2291.
- [8] Etaati GR, Amrollahi R, Habibi M, Mohammadi K, Baghdadi R, Roomi A. Study of the soft and hard x-ray emitted by APF plasma focus device in different pressures. *Journal of Fusion Energy* 2010; 29(5): 503-507.
- [9] Ng CM, Moo SP, Wong CS. Variation of the soft x-ray emission with gas pressure in a plasma focus. *IEEE Transactions on Plasma Science* 1998; 26(4): 1146-1153.
- [10] Roomi A, Saion E, Habibi M, Amrollahi R, Baghdadi R, Etaati GR, Mahmood W, Iqbal M. The effect of applied voltage and operating pressure on emitted x-ray from nitrogen (n2) gas in APF plasma focus device. *Journal of Fusion Energy* 2011; 30(5): 413-420.
- [11] Ay Y, Al-Halim MAA, Bourham MA. Simulation of the plasma sheath Dynamics in a spherical plasma focus. *The European Physical Journal D* 2015; 69(9).
- [12] Ay Y, Al-Halim MAA, Bourham MA. MHD simulation for neutron yield, radiations and beam-ion properties in the spherical plasma focus. *Journal of Fusion Energy* 2015; 35(2): 407-414.

- [13] Ay Y. A neutron source with 10¹⁴ DT neutron yield. *International Journal of Modern Physics E* 2020; 28(11): 1950097.
- [14] Ay Y. A Neutron Source With 10¹³ Neutron Yield and Ion Properties With Respect to Gas Pressure in a Spherical Plasma Focus, *IEEE Transactions on Plasma Science* 2020; 48(3): 700-705.
- [15] Ay Y. Effect of the cathode radius on plasma dynamics and radiation emissions in a spherical plasma focus device. *Physics of Plasmas* 2019; 26 (10): 102506.